東京大学　生産技術研究所
北條　博彦

化学生命工学専攻

有機機能材料学特論II

励起状態のモデル化

配置換相互作用法
Configuration Interaction (CI) Method

- Full-CI （現実的でない）
- CI-Singles （配置の選び方に依存）

時間発展法
Time-Propagation Method

- 時間依存Hartree-Fock
- 時間依存DFT
  - 時間依存Schrödinger方程式
  - 密度汎関数理論（DFT）

配置間相互作用

励起（主に価電子の一電子励起）状態のエネルギーを求める→基底状態との差が吸収波長に相当

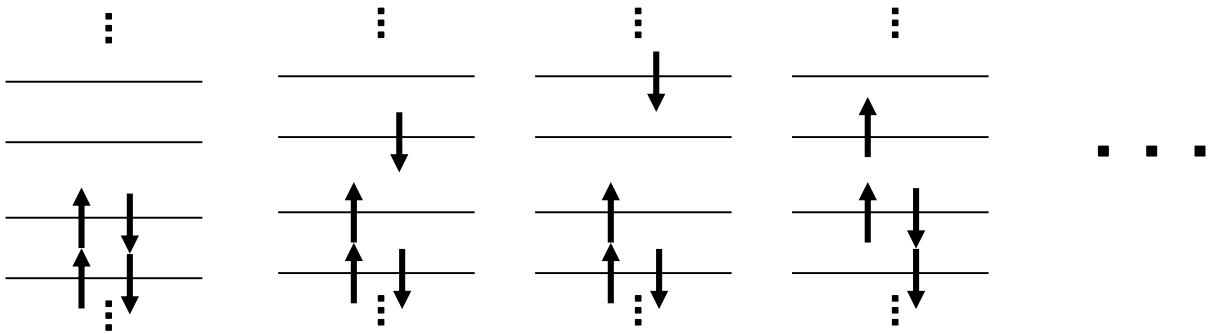

Ψ_0　Φ_1　Φ_2　Φ_3　**→Slater行列式で表現**

$$\Psi_k = \sum_i A_{ki} \Phi_i$$

$$\sum_j A_{kj} \left(H_{ij} - E S_{ij} \right) = 0$$

$$H_{ij} = \int \Phi_i^* \hat{H} \Phi_j \, \mathrm{d}v, \quad S_{ij} = \int \Phi_i^* \Phi_j \, \mathrm{d}v$$

配置間相互作用
(Configuration Interaction, CI)

時間依存Schrödinger方程式

$$i\hbar\frac{\partial}{\partial t}\left|\psi(t)\right\rangle = \hat{H}\left|\psi(t)\right\rangle$$

Hは時間を推進する

$$\left|\psi(t)\right\rangle = \exp\left[-\frac{i}{\hbar}\hat{H}t\right]\left|\psi(0)\right\rangle$$

$$\left|\psi(t+\Delta t)\right\rangle = \exp\left[-\frac{i}{\hbar}\hat{H}\Delta t\right]\left|\psi(t)\right\rangle$$

$$\exp\hat{A} = 1+\hat{A}+\frac{1}{2!}\hat{A}^2+\cdots+\frac{1}{n!}\hat{A}^n+\cdots \equiv U$$

AがHermitであればexpAはUnitary

選択律は時間に依存する摂動論で導かれる

時間依存Schrödinger方程式　$\hat{H}\Psi = i\hbar\dfrac{\partial\Psi}{\partial t},\quad \Psi_n(r,t) = \psi_n(r)\exp\left[-i\dfrac{E_n t}{\hbar}\right]$

電磁場による摂動　$E = E_0\cos 2\pi\nu t,\quad \hat{H}^{(1)} = -\mu\cdot E = -\mu\cdot E_0\cos 2\pi\nu t$

二状態モデル　$\Psi_1(t) = \psi_1\exp\left[-i\dfrac{E_1 t}{\hbar}\right],\ \Psi_2(t) = \psi_2\exp\left[-i\dfrac{E_2 t}{\hbar}\right]$

$\hat{H} + \hat{H}^{(1)}\Psi = i\hbar\dfrac{\partial\Psi}{\partial t}$ に　$\Psi = a_1(t)\Psi_1 + a_2(t)\Psi_2$ を代入すると、

$$\hat{H}^{(1)}\left(a_1\exp\left[-i\frac{E_1}{\hbar}t\right]\psi_1 + a_2\exp\left[-i\frac{E_2}{\hbar}t\right]\psi_2\right)$$

$$= i\hbar\left(\frac{\partial a_1}{\partial t}\right)\exp\left[-i\frac{E_1}{\hbar}t\right]\psi_1 + i\hbar\left(\frac{\partial a_2}{\partial t}\right)\exp\left[-i\frac{E_2}{\hbar}t\right]\psi_2$$

（つづき）

Ψ_2^* をかけて積分し、$a_1(0)=1,\ a_2(0)=0$ とすると、$t=0$において、

$$\frac{\partial a_2}{\partial t}=-\frac{i}{\hbar}\exp\left[i\frac{(E_2-E_1)}{\hbar}t\right]\int\psi_2^*\hat{H}^{(1)}\psi_1\,\mathrm{d}\tau$$

$$a_2(t)=-\frac{i}{2\hbar}(\mu_z)_{12}E_{0z}\int_0^t\left\{\exp\left[i\frac{(E_2-E_1+h\nu)t'}{\hbar}\right]+\exp\left[i\frac{(E_2-E_1-h\nu)t'}{\hbar}\right]\right\}\mathrm{d}t'$$

$$=\frac{1}{2}(\mu_z)_{12}E_{0z}\left\{\frac{1-\exp\left[-i\dfrac{(E_2-E_1-h\nu)t}{\hbar}\right]}{E_2-E_1-h\nu}\right\}$$

ここで、遷移双極子モーメントを

$$(\mu_z)_{12}=\int\psi_2^*\mu_z\psi_1\,\mathrm{d}\tau$$

と定義した

$$a_2^*(t)a_2(t)=\left|(\mu_z)_{12}\right|^2{E_{0z}}^2\frac{\sin^2\left[\dfrac{(E_2-E_1-h\nu)t}{2\hbar}\right]}{(E_2-E_1-h\nu)^2}$$

$$\mathrm{sinc}\,(x)=\frac{\sin x}{x}$$

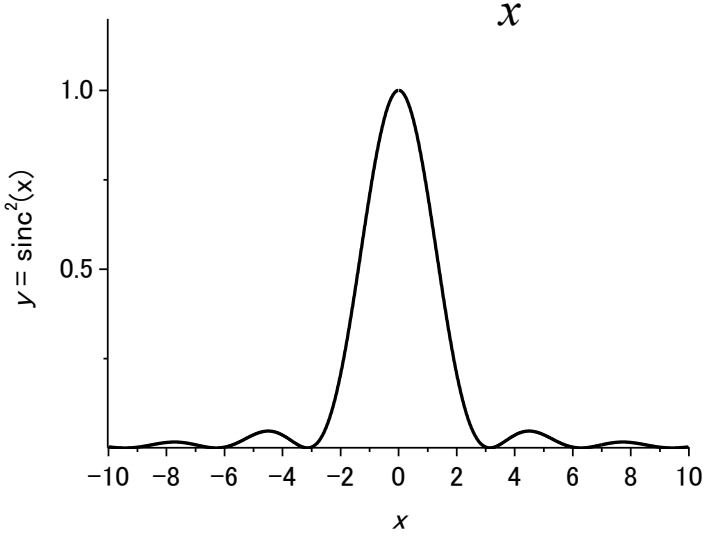

$$U_{\mathrm{f}} = \frac{\pi e^2 F_0^2}{4m}$$

$$f = \frac{U}{U_{\mathrm{f}}} = \frac{8m}{e^2 \hbar^2 F_0^2} \Delta E \left| V_{\mathrm{BA}} \right|^2$$

$$f = \frac{8m}{e^2 \hbar^2} \Delta E \left| \mu_{\mathrm{BA}} \right|^2$$

$$p(\omega) = 10^{-1} \times \ln 10 \times \frac{\varepsilon(\omega) c_0 \rho}{N_{\mathrm{A}}}$$

$$u(\omega) = \frac{1}{2} c_0 \varepsilon_0 F_0^2 = \hbar \omega c_0 \rho$$

$$f = \frac{4m}{\pi e^2 F_0^2} \hbar\omega \int p(\omega) \mathrm{d}\omega = 10^{-1} \times \ln 10 \times \frac{2 c_0 \varepsilon_0 m}{\pi e^2 N_{\mathrm{A}}} \int \varepsilon(\omega) \mathrm{d}\omega$$

$$f = 10^8 \times \ln 10 \times \frac{4 c_0^2 \varepsilon_0 m}{e^2 N_{\mathrm{A}}} \int \frac{\varepsilon(\lambda)}{\lambda^2} \mathrm{d}\lambda = 4.32 \times 10^{-2} \times \int \frac{\varepsilon(\lambda)}{\lambda^2} \mathrm{d}\lambda$$

密度汎関数法

Density Functional Theory

Hohenberg-Kohn定理

基底状態の波動関数は電子密度分布と1対1に対応する

Kohn-Sham方程式

$$\left[-\frac{1}{2}\nabla^2 + V_{\mathrm{KS}}(\hat{r})\right]\varphi_i(r) = \varepsilon_i \varphi_i(r)$$

$\varphi_i(r)$: 仮想電子波動関数

$$\rho(r) = 2\sum_{i=1}^{n}\left|\varphi_i(r)\right|^2$$

V_H: Hartreeポテンシャル
V_{XC}: 交換相関ポテンシャル
V_{ext}: 外場ポテンシャル

$$V_{\mathrm{KS}} = V_{\mathrm{H}}[\rho(r)] + V_{\mathrm{XC}}[\rho(r)] + V_{\mathrm{ext}}[\rho(r)]$$

時間依存密度汎関数法

Runge-Gross定理

時間依存の波動関数は電子密度分布と1対1に対応する

時間依存Kohn-Sham方程式

$$\left[-\frac{1}{2}\nabla^2 + V_{\mathrm{KS}}(\hat{r})\right]\varphi_i(r,t) = i\frac{\partial}{\partial t}\varphi_i(r,t)$$

基底状態を初期値とし、V_{ext}として振動電場を考えてρ(r,t)を時間発展させる

→励起状態のρ(r,t)と励起エネルギー、振動子強度などがわかる。

励起状態の計算

```
%chk=default
```
チェックポイントファイルの指定

```
#N B3LYP/6-311G** TD=(Nstates=5)
```
時間依存DFT

```
water molecule
```
コメント

```
0 1
O
H 1 r2
H 1 r3   2 a3

r2 1.0
r3 1.0
a3 104.5
```
電荷、スピン多重度
構造情報

通常のDFT計算の結果

```
 Initial guess orbital symmetries:
        Occupied  (A1) (A1) (B2) (A1) (B1)
        Virtual   (A1) (B2) (B2) (A1) (B1) (A1) (B2) (A1) (A1) (A2)
                  (B1) (B2) (B2) (A1) (A1) (B2) (B1) (A2) (A1) (A1)
                  (B2) (B1) (A1) (B2) (A1)
  The electronic state of the initial guess is 1-A1.
  Requested convergence on RMS density matrix=1.00D-08 within 128 cycles.
  Requested convergence on MAX density matrix=1.00D-06.
  Requested convergence on                 energy=1.00D-06.
  No special actions if energy rises.
  Keep R1 integrals in memory in canonical form, NReq=      614236.
  Integral accuracy reduced to 1.0D-05 until final iterations.
  Initial convergence to 1.0D-05 achieved.  Increase integral accuracy.
  SCF Done:  E(RB+HF-LYP) =  -76.4459738120     A.U. after    9 cycles
              Convg  =    0.9400D-08             -V/T =  2.0028
              S**2   =   0.0000
ExpMin= 1.03D-01 ExpMax= 8.59D+03 ExpMxC= 1.30D+03 IAcc=1 IRadAn=         1 AccDes=
1.00D-06
  HarFok:  IExCor= 205 AccDes= 1.00D-06 IRadAn=         1 IDoV=1
  ScaDFX=  1.000000  1.000000  1.000000  1.000000
  Range of M.O.s used for correlation:     2    30
  NBasis=    30 NAE=     5 NBE=     5 NFC=     1 NFV=     0
  NROrb=     29 NOA=     4 NOB=     4 NVA=    25 NVB=    25
  R1, R2, and R3 integrals will be kept in memory, NReq=      799768.
  Orbital symmetries:
        Occupied  (A1) (A1) (B2) (A1) (B1)
        Virtual   (A1) (B2) (B2) (A1) (A1) (B1) (B2) (A1) (A1) (A2)
                  (B1) (B2) (B2) (A1) (A1) (B2) (B1) (A2) (A1) (A1)
                  (B2) (B1) (A1) (B2) (A1)
```

励起状態の計算結果

```
20 initial guesses have been made.
Convergence on wavefunction:    0.001000000000000
Iteration     1 Dimension    20 NMult    20
CISAX will form  20 AO SS matrices at one time.
Iteration     2 Dimension    30 NMult    30
Iteration     3 Dimension    40 NMult    40
Iteration     4 Dimension    44 NMult    44
*****************************************************************
Excited states from <AA,BB:AA,BB> singles matrix:
*****************************************************************

Ground to excited state Transition electric dipole moments (Au):
      state          X           Y           Z          Osc.
        1         0.3692      0.0000      0.0000      0.0238
        2         0.0000      0.0000      0.0000      0.0000
        3         0.0000      0.0000      0.6169      0.0904
        4         0.0000      0.4270      0.0000      0.0519
        5         0.0000      0.8867      0.0000      0.2501
Ground to excited state transition velocity dipole Moments (Au):
      state          X           Y           Z          Osc.
        1        -0.2005      0.0000      0.0000      0.1022
        2         0.0000      0.0000      0.0000      0.0000
        3         0.0000      0.0000     -0.2903      0.1576
        4         0.0000     -0.1762      0.0000      0.0485
        5         0.0000     -0.4169      0.0000      0.2428
```

Ground to excited state transition magnetic dipole Moments (Au):

state	X	Y	Z
1	0.0000	0.1874	0.0000
2	0.0000	0.0000	-0.2790
3	0.0000	0.0000	0.0000
4	0.2776	0.0000	0.0000
5	-0.0895	0.0000	0.0000

<0|del|b> * <b|rxdel|0> (Au), Rotatory Strengths (R) in cgs (10**-40 erg-esu-cm/Gauss)

state	X	Y	Z	R(velocity)
1	0.0000	0.0000	0.0000	0.0000
2	0.0000	0.0000	0.0000	0.0000
3	0.0000	0.0000	0.0000	0.0000
4	0.0000	0.0000	0.0000	0.0000
5	0.0000	0.0000	0.0000	0.0000

<0|r|b> * <b|rxdel|0> (Au), Rotatory Strengths (R) in cgs (10**-40 erg-esu-cm/Gauss)

state	X	Y	Z	R(length)
1	0.0000	0.0000	0.0000	0.0000
2	0.0000	0.0000	0.0000	0.0000
3	0.0000	0.0000	0.0000	0.0000
4	0.0000	0.0000	0.0000	0.0000
5	0.0000	0.0000	0.0000	0.0000

<0|del|b> * <b|r|0> (Au)

state	X	Y	Z	Osc.(frdel)
1	-0.0740	0.0000	0.0000	0.0494
2	0.0000	0.0000	0.0000	0.0000
3	0.0000	0.0000	-0.1791	0.1194
4	0.0000	-0.0752	0.0000	0.0501
5	0.0000	-0.3697	0.0000	0.2464

Ground to excited state transition densities written to RWF 633

励起配置・吸収波長・振動子強度など

```
Excitation energies and oscillator strengths:

Excited State   1:   Singlet-B1     7.1349 eV  173.77 nm  f=0.0238
      5 ->  6         0.69252
This state for optimization and/or second-order correction.
Copying the excited state density for this state as the 1-particle RhoCI density.

Excited State   2:   Singlet-A2     9.0146 eV  137.54 nm  f=0.0000
      5 ->  7         0.70011

Excited State   3:   Singlet-A1     9.7004 eV  127.81 nm  f=0.0904
      4 ->  6         0.68703

Excited State   4:   Singlet-B2    11.6169 eV  106.73 nm  f=0.0519
      4 ->  7         0.68969

Excited State   5:   Singlet-B2    12.9866 eV   95.47 nm  f=0.2501
      3 ->  6         0.68673
```

Inorganic Chemistry

ARTICLE

pubs.acs.org/IC

Comparison of the Spectroscopic Properties of π-Conjugated, Fused Salphen Triads Embedded with Zn-Homo-, Ni-Homo-, and Ni/Zn-Heteronuclei

Hirohiko Houjou,* Muneyuki Ito, and Koji Araki

Institute of Industrial Science, The University of Tokyo, 4-6-1 Komaba, Meguro-ku, Tokyo 153-8505, Japan

Supporting Information

Inorg. Chem. **50** (2011) 5298-5306.

ABSTRACT: Stepwise condensation reactions of 2,6-dihydroxynaphthalene-1,5-dicarbaldehyde and a phenylenediamine with concomitant binding of metal ions afforded a trinuclear complex of a fully π-conjugated, fused salphen ligand. By changing the synthetic pathway, we obtained a series of homo- and heteronuclear complexes containing selected combinations of nickel(II) and zinc(II) ions. Comparison of the trinuclear complexes' spectroscopic features with those of analogous dinuclear complexes revealed that the absorption spectrum of each trinuclear complex is composed of a salphen-centered absorption at 400 nm and a naphthalene-centered absorption around 500−600 nm, suggesting that the π-conjugated system is divided into several compartments, each of which independently undergoes electronic excitation. Molecular orbital calculations revealed that the formal fusion of the salphen moieties increases the highest occupied molecular orbital (HOMO) level by ~0.4 eV, which in turn causes the low-energy absorption observed in the spectra. In contrast, interorbital interactions mediated by the N_2O_2 metal coordination site are small, even though this site is bridged by an *o*-phenylene linkage. These results suggest that the coordination site effectively breaks electronic communication between the compartments, which in turn affect various spectroscopic properties of the π-conjugated metallo-polysalphens.

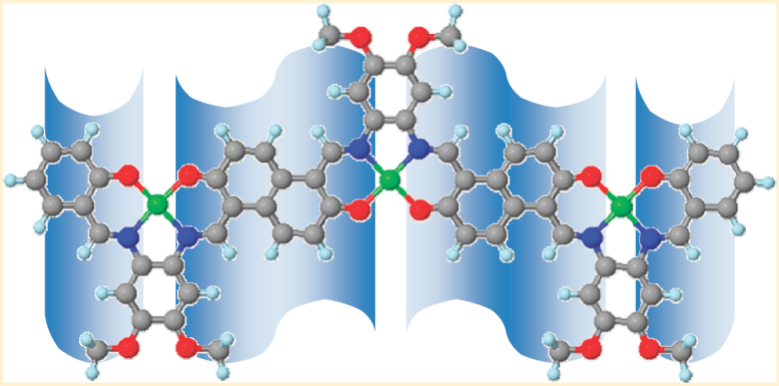

Scheme 1. Synthesis of the Trinuclear Complex $M_aM_bM_aL3$

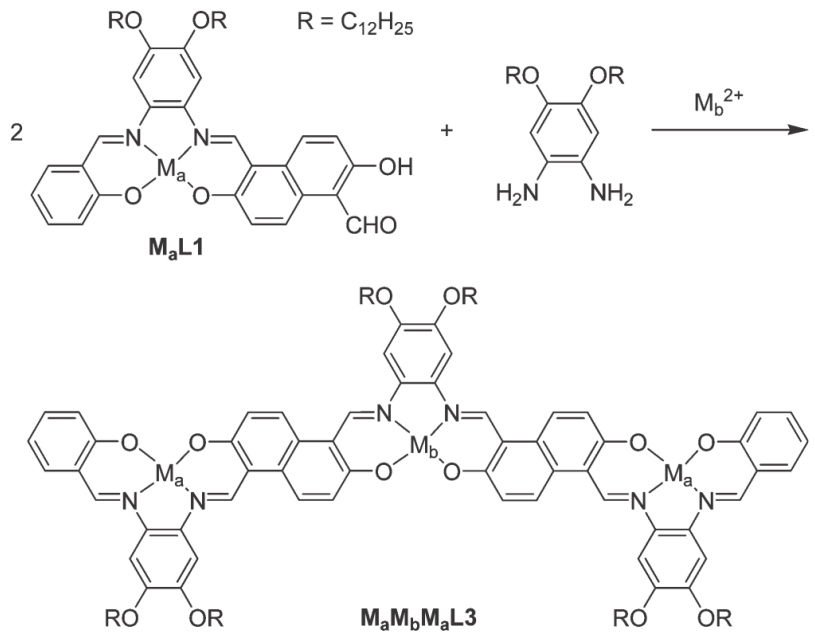

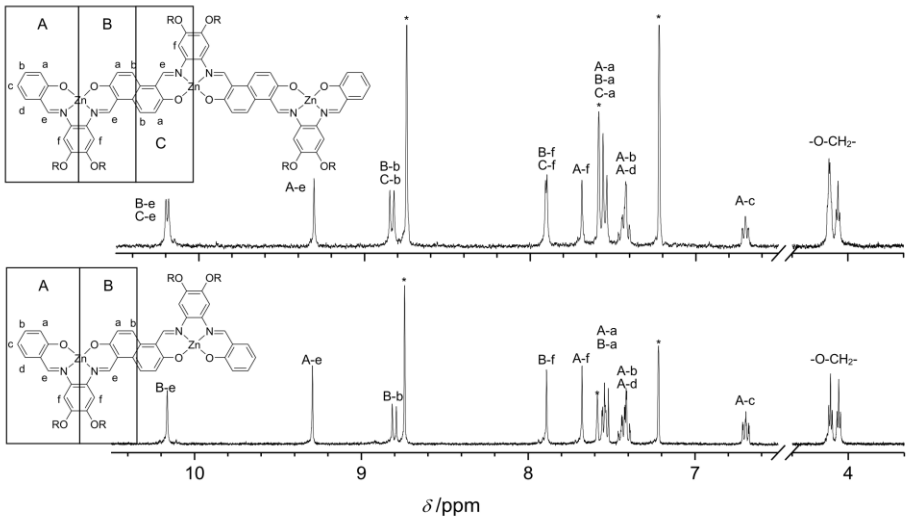

Figure S2 Comparison of ^{1}H NMR spectra of Zn_3L3 and Zn_2L2 (*: solvent (pyridine))

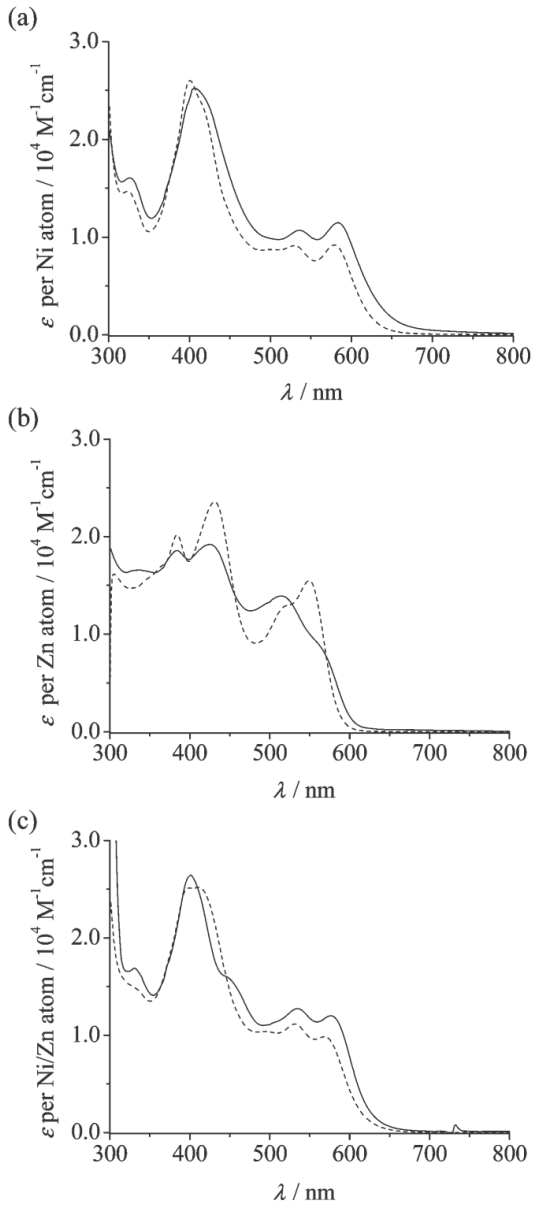

Figure 3. UV−vis absorption spectra of trinuclear (solid line) and dinuclear (dashed line) complexes: (a) Ni_3L3 and Ni_2L2, (b) Zn_3L3 and Zn_2L2, and (c) NiZnNiL3 and NiZnL2. Absorption coefficients are normalized by the number of metal atoms per molecule.

Table 2. Selected Data for the Results of SCI Calculation of Di- and Trinuclear Salphen Complexes

	$\lambda_{calcd.}$/nm (state)	dominant contributions (CI coefficients)	oscillator strength
Ni_2L2	464 (^1B_u)	143→146 (−0.20)	0.56
		144→145 (0.60)	
	401 (^1B_u)	142→145 (−0.31)	1.10
		142→147 (0.31)	
		143→146 (0.37)	
	355 (^1B_u)	140→145 (0.39)	0.99
		142→145 (−0.30)	
Ni_3L3	473 ($^1B_1$)	212→215 (−0.37)	0.68
		213→214 (0.49)	
	452 ($^1A_1$)	212→214 (0.43)	0.49
		213→215 (−0.39)	
	408 ($^1A_1$)	210→214 (0.22)	0.96
		210→216 (0.22)	
		211→215 (−0.22)	
		211→217 (0.22)	
		212→216 (0.23)	
	396 ($^1B_1$)	210→217 (0.29)	0.11
		211→216 (0.30)	
	391 ($^1A_1$)	211→217 (0.23)	0.27
		212→218 (0.29)	
		213→219 (0.28)	
	361 ($^1B_1$)	207→214 (0.30)	1.52
		208→215 (0.21)	
		209→214 (0.26)	
	352 ($^1A_1$)	207→215 (0.24)	0.34
		209→215 (0.22)	

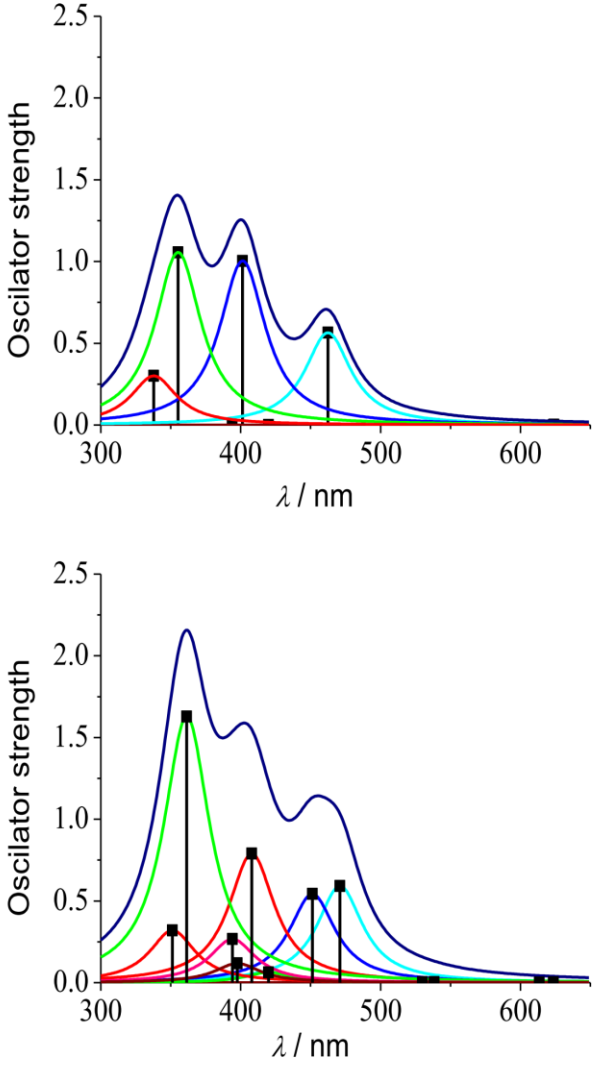

Figure S4 Absorption profiles of (a) Ni2L2 and (b) Ni3L3 simulated using the results of ZINDO calculations. A Lorentzian curve was applied to each excitation.

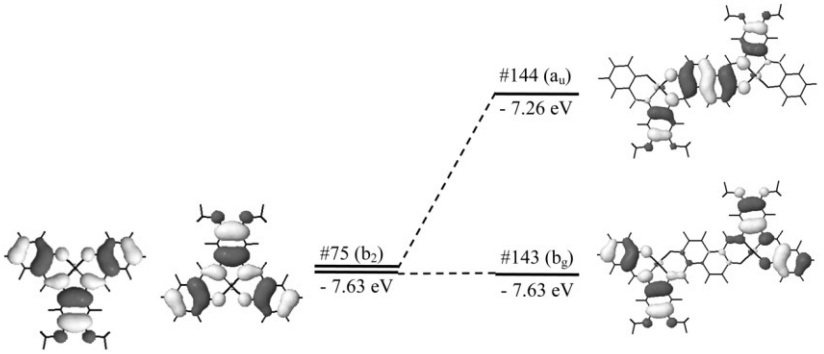

Figure 4. Schematic representation of interorbital interaction that generates near-HOMO orbitals of Ni 2 L2.

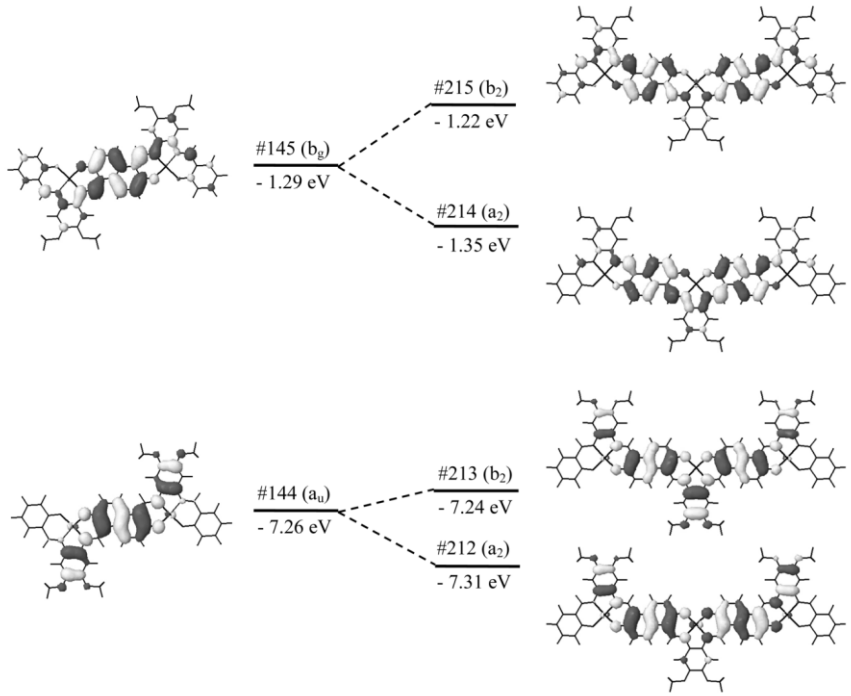

Figure 5. Schematic representation of the correlation diagram of the near-HOMO/LUMO orbitals between di- and trinuclear nickel complexes.

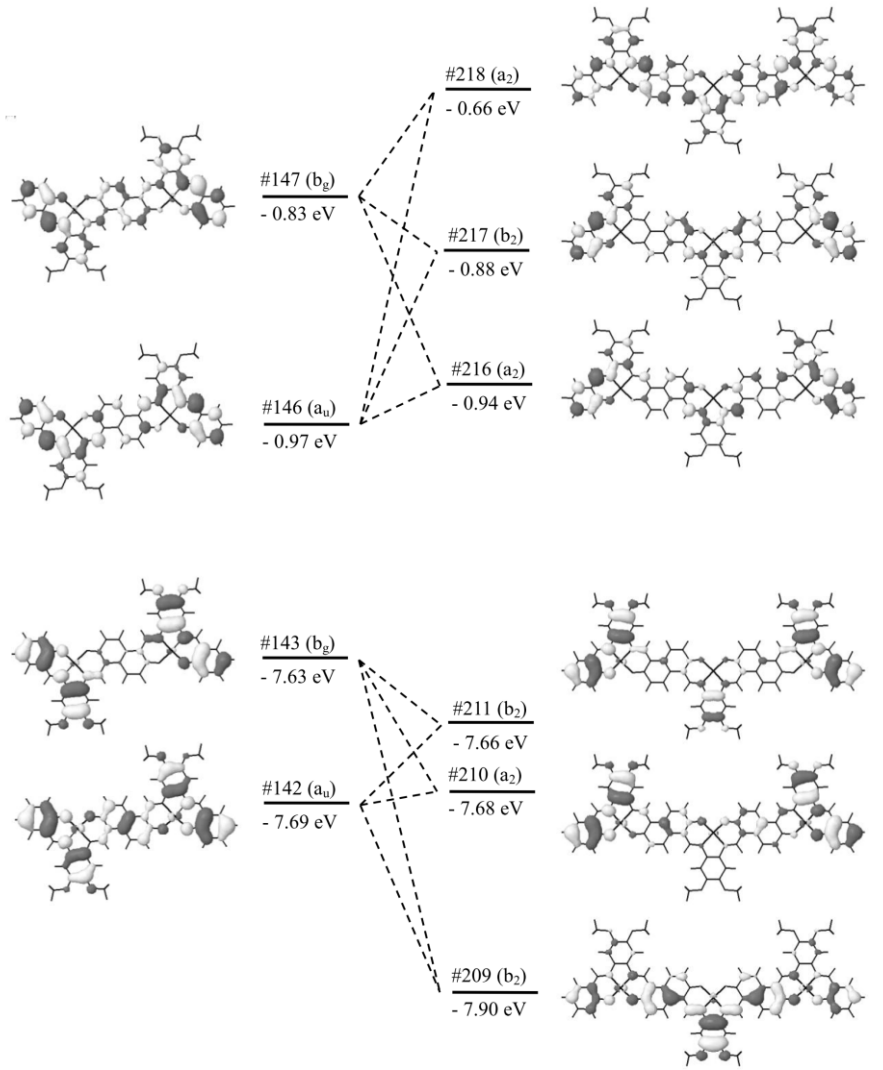

Figure S5 Schematic representation of the correlation diagram of the under-HOMO/over-LUMO orbitals between di- and tri-nuclear nickel complexes